Range-Free Localization With a Mobile Beacon via Motion Compensation in Underwater Sensor Networks

Yonghun Kim, *Student Member, IEEE*, Melike Erol-Kantarci, *Senior Member, IEEE*, Youngtae Noh, *Member, IEEE*, and Kiseon Kim, *Senior Member, IEEE*

***Abstract*—Localization accuracy is crucial for achieving reliable location tagging for underwater missions. However, the accuracy of conventional range-free localization schemes with a mobile beacon is distorted by ship dynamics (*i.e.*, pitch, roll, and heave) over oceanic conditions, and the schemes suffer from two uncertainties: beacon point and geometric shape uncertainties. To reduce the effects of these uncertainties, we herein propose LMB-MC, a novel range-free localization scheme. LMB-MC compensates beacon point errors and employs an accurate geometric model instead of an unconditional circle-shaped model. Furthermore, we adopted real-world motion measurements from an operating ship and used motion data to support diverse simulation settings (*i.e.*, Douglas sea scales). Result of extensive simulation studies verified that LMB-MC provided improved accuracy and reliability compared to the existing solutions in the considered oceanic environments.**

***Index Terms*—Douglas sea scale, range-free, localization, mobile beacon, motion compensation, UASNs.**

I. Introduction

In THE last decade, localization techniques for underwater acoustic sensor networks (UASNs) have been widely studied to support diverse location-based applications, such as oceanographic monitoring systems, offshore exploration, tactical surveillance, and disaster prevention [1]. For enabling such applications, geometric constraint-based range-free localization has been proposed due to its computational simplicity and energy efficiency [2]. Furthermore, instead of static anchor nodes, a mobile beacon—a ship or an autonomous underwater vehicle (AUV)—has been widely used [3] owing to its flexibility (*i.e.*, wider coverage) and efficiency (*i.e.*, smaller number of high-end anchor nodes).

Recently, Luo *et al.* proposed a range-free localization with directional beacons (LDB) scheme for UASNs [4], and reported its improved accuracy and effectiveness based on geometric constraints. However, the scheme simply computes location of the sensor nodes with selected beacon points; hence, its localization accuracy is sensitively degraded by increased errors because of the beacon points. To address this drawback, Lee and Kim proposed localization with a mobile beacon (LoMoB) [5]. Compared to LDB, LoMoB considered all potential points (*i.e.*, valid intersections) formed by the beacon points and computed the locations of sensor nodes from the weighted mean of potential points. Hence, LoMoB outperforms LDB in terms of accuracy and reliability.

However, all these schemes do not comprehensively consider the dynamics of a mobile beacon (*i.e.*, pitch, roll, and heave [3]), that consistently change over time owing to the effect of oceanic waves on the sea surface or underwater oceanic currents [6]. This hinders the practicability of such schemes in real-world deployment. When launching a beam from a directional transceiver over oceanic waves, the beam angle changes significantly, which results in two major uncertainties: *beacon point uncertainty* (*i.e.*, confusion regarding beacon points due to changes in beam angle), and *geometric shape uncertainty* (*i.e.*, confusion between a circle and an ellipse). Because of these two uncertainties, the performance of existing schemes is severely degraded, making them inapplicable in real-world settings.

Hence, we herein propose Localization with a Mobile Beacon via Motion Compensation (LMB-MC), a novel range-free localization scheme that overcomes the aforementioned uncertainties by considering the motion compensation. The proposed scheme compensates for the uncertainties in beacon points by using the measured motion of the ship/AUV and addresses the geometric shape uncertainty by employing an accurate ellipse-based model. In real-world environments, LMB-MC reduces the error effect from the ship dynamics and outperforms the existing schemes in terms of localization accuracy. The contributions of this letter are as follows:

- We proposed LMB-MC, a novel range-free localization scheme via motion compensation. This scheme reduces beacon point uncertainty by compensating the passive motion of the ship and geometric shape uncertainty by employing a more accurate ellipse-based model.
- To evaluate the LMB-MC's performance and compare it to the state-of-the-art schemes (*i.e.*, LoMoB and LDB) in

Manuscript received July 16, 2020; accepted August 12, 2020. Date of publication August 18, 2020; date of current version January 8, 2021. This work was suppored in part by the SAVEX15 data was provided by KRISO under Grant PES1940, in part by KIOST under Grant PE99331, in part by MPL and ONR under Grant N00014-31-1-0510, in part by the 'Development of Ocean Acoustic Echo Sounder and Hydro-Physical Properties Monitoring Systems,' funded by the Ministry of Oceans and Fisheries, South Korea, and in part by the Basic Science Research Program through the National Research Foundation of Korea (NRF) funded by the Ministry of Education under Grant NRF-2019R1F1A1059898. The associate editor coordinating the review of this article and approving it for publication was S. Ma. *(Corresponding authors: Kiseon Kim; Youngtae Noh.)*

Yonghun Kim and Kiseon Kim are with the School of Electrical Engineering and Computer Science, Gwangju Institute of Science and Technology, Gwangju 61005, South Korea (e-mail: mizpah@gist.ac.kr; kskim@gist.ac.kr).

Melike Erol-Kantarci is with the School of Electrical Engineering and Computer Science, University of Ottawa, Ottawa, ON KIN 6N5, Canada (e-mail: melike.erolkantarci@uottawa.ca).

Youngtae Noh is with the Department of Computer Engineering, Inha University, Incheon 22212, South Korea (e-mail: ytnoh@inha.ac.kr).

Digital Object Identifier 10.1109/LWC.2020.3017520

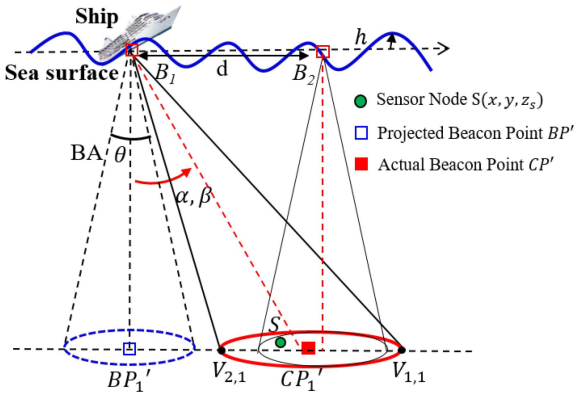

Fig. 1. System environment with a mobile beacon and the effect of change in ship dynamics over the sea surface.

various settings, we use ship motion data obtained from real-world measurements (SAVEX15 [7]) and further model oceanic conditions to consider dynamic scenarios. Finally, we verified the improved accuracy of LMB-MC over that of the existing schemes in the considered oceanic environments.

II. LMB-MC Localization Scheme

In this section, we first define the localization problem in underwater environments and describe the procedure of our proposed scheme.

A. Localization Problem and Assumptions

We consider a range-free localization system with a mobile beacon (*i.e.*, ship/AUV) equipped with a directional transceiver. As shown in Fig. 1, the mobile beacon can maneuver on the sea surface or underwater at a fixed depth z_a following a predefined path. By following the path, the mobile beacon broadcasts acoustic beacon signals (B_i) at regular intervals (*e.g.*, every second) with a beacon distance (BD, d) between B_1 and B_2, and the beam angle (BA, θ) of the transceiver, and the motions (*i.e.*, pitch α to transverse axis, roll β to longitudinal axis, and heave h). To collect underwater sensing data, sensor nodes $S(x, y, z_s)$ are randomly deployed underwater at different depths. For location tagging, the sensor nodes passively receive the beacon signals B_i from the mobile beacon, and use a projection technique (*i.e.*, transforming a 3D problem into a 2D problem) to localize its location by directly obtaining its depth information z_s from a pressure sensor [1]. To select beacon points among the received beacons, the first-heard and last-heard beacon points are used as reference points (*e.g.*, B_1 and B_2 on a path-line in Fig. 1, respectively) to generate geometries for localization as in [4], [5].

To localize a sensor node in range-free localization schemes (*i.e.*, LoMoB and LDB), two processes are required: beacon point selection and location computation. However, the BA might change considerably because of the oceanic waves; therefore, each process involves considerable errors due to the effects of the two uncertainties, i.e., *beacon point uncertainty* and *geometric shape uncertainty*. Our main objective is to reliably reduce the uncertainties by beacon point and geometric shape compensations.

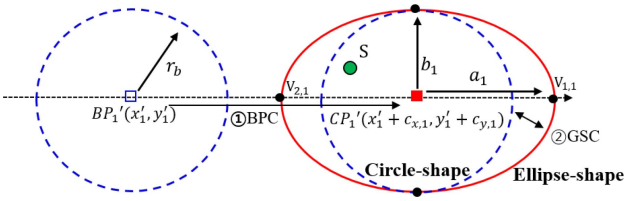

Fig. 2. Phases (BPC and GSC) of LMB-MC with a received beacon (B_1) on a horizontal plane (at z_s from the viewpoint of a located sensor node).

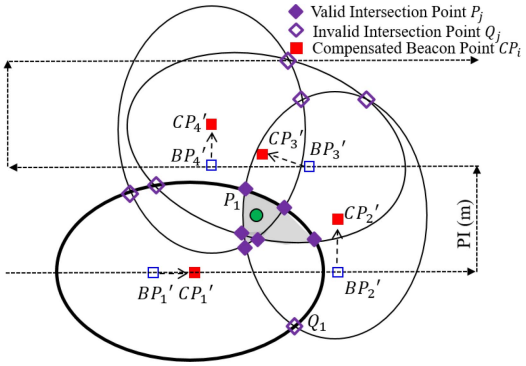

Fig. 3. Elliptical location computation of LMB-MC on a horizontal plane (at z_s from the viewpoint of a located sensor node) with ship movement on the sea surface (at $z_a = 0$).

B. Procedure of the Proposed Scheme

1) Beacon Point Compensation (BPC): For beacon point selection, as shown in Fig. 2, the prevalent range-free schemes naively use the i^{th} beacon points ($BP_i'(x_i', y_i')$) projected onto a horizontal plane (*i.e.*, at z_s, the viewpoint of a located sensor node) from the received beacons, regardless of changes in the direction of the transmitted beam caused by ship dynamics. Since the actual beacon point is located at the center of ellipse ($CP_i'(x_i' + c_{x,i},\ y_i' + c_{y,i})$, where $c_{x,i}$ and $c_{y,i}$ are the i^{th} displacement from x_i' and y_i', respectively), the localization accuracy of the schemes can be degraded severely. To overcome this limitation (*i.e.*, beacon point uncertainty), the dynamics of a ship over the oceanic waves must be considered, and the shifts $c_{x,i}$ and $c_{y,i}$ must be compensated to correctly compute CP_i' to be an accurate reference point. To compute CP_i' in the BPC phase, we must compensate for the effects on the BAs caused by ship dynamics, (*i.e.*, pitch α_i and roll β_i). For pitch compensation, the coordinates of the two vertices (*i.e.*, $V_{1,i}$, $V_{2,i}$) can be represented as $z_d \times \tan(\alpha_i + \theta_i/2)$ and $z_d \times \tan(\alpha_i - \theta_i/2)$, where z_d is the difference depth between z_s and z_a (*i.e.*, $z_d = |z_s - z_a|$). The displacement $c_{x,i}$ from x_i' can be expressed as $z_d \times (\frac{\tan(\alpha_i+\theta_i/2)+\tan(\alpha_i-\theta_i/2)}{2})$. Similarly, for roll compensation, $c_{y,i}$ can be expressed as $z_d \times (\frac{\tan(\beta_i+\theta/2)+\tan(\beta_i-\theta/2)}{2})$. By performing BPC, we can correctly compute the i^{th} compensated beacon point CP_i'.

2) Geometric Shape Compensation (GSC): For accurate location computation, an appropriate geometric model is crucial in order to draw the valid intersection area (*i.e.*, the gray shaded area in Fig. 3). However, as shown in Fig. 2, the existing schemes assume a circle-shape model with fixed radius

(r_b) at all times; in turn, the location performance can be affected owing to the misleading geometric shapes by abrupt BA changes (*i.e.*, geometric shape uncertainty). To reduce this uncertainty, in the GSC phase, we adopt a generic ellipse shape of radius a_i on the x-axis and b_i on the y-axis (which are the semi-major and semi-minor axes of the i^{th} ellipse, respectively), at a depth z_s. As discussed in the previous phase, the center of ellipse (CP_i') is compensated at the coordinate $(x_i' + c_{x,i}, y_i' + c_{y,i})$ from the projected beacon point $(BP_i'(x_i', y_i'))$. Therefore, the overall geometric shape model can be expressed as follows:

$$\frac{(x_i' - c_{x,i})^2}{a_i^2} + \frac{(y' - c_{y,i})^2}{b_i^2} = 1. \quad (1)$$

The semi-major radius a_i can be calculated as the difference between the location of the maximum vertex and the center of the ellipse, i.e., $z_d \times (\frac{\tan(\alpha_i+\theta/2)-\tan(\alpha_i-\theta/2)}{2})$. Similarly, the semi-minor radius b can be calculated as $z_d \times (\frac{\tan(\beta_i+\theta/2)-\tan(\beta_i-\theta/2)}{2})$.

3) Elliptical Location Computation: As shown in Fig. 3, according to a predefined mobile path and a series of the received beacon signals, we can select *N* beacon points as reference points for location computation and construct *N* ellipses with its valid intersection points on a horizontal plane (at z_s). After BPC and GSC phases, the location of the target node can be calculated using the following equations:

$$\sqrt{\frac{(x - (x_i' + c_{x,i}))^2}{{a_i}^2} + \frac{(y - (y_i' + c_{y,i}))^2}{{b_i}^2}} = 1, \quad (2)$$

where (x, y) is the coordinate of a sensor node. Based on this equation, we can obtain the valid potential points P_j among the $N(N-1)$ intersection points by a bilateration method (*i.e.*, selecting closer points P_j instead of Q_j in Fig. 3) [2]. By taking the mean of the all N_p potential points, the estimated location $(\hat{x}, \hat{y})$ can be computed as in [5], $(\hat{x}, \hat{y}) = (\sum_{j=1}^{N_P} \hat{x}_{p,j}/N_p, \sum_{j=1}^{N_P} \hat{y}_{p,j}/N_p)$, where N_p is the number of the potential points $N(N-1)/2$. In certain circumstances, sensor nodes may not receive enough beacon signals (*i.e.*, $N < 3$). To handle these cases, LMB-MC estimates the location of the sensor nodes as the midpoints of the intersections points (P_j and Q_j, $N = 2$) or estimates the location of the nodes as the beacon point itself ($N = 1$).

The major departure of LMB-MC from existing schemes is in two manners, namely, the adoption of the compensated beacon points and the consideration of the ellipse geometries instead of naive circle-based geometries for the beacon projections. This will result in enhanced accuracy especially in a harsh oceanic environment (*i.e.*, beam angle changes due to the severe ship dynamics).

III. Ship Motion Dataset and Modeling

In this section, we use a ship motion measurement dataset obtained from Shallow-water Acoustic Variability Experiment (SAVEX15 in [7]) to apply a realistic motion model to our extensive simulation. SAVEX15 was conducted to measure the environmental data and to analyze acoustic signals for scientific purposes in shallow water (*i.e.*, approximately 100 m deep) near Jeju Island in South Korea. For SAVEX15, the R/V Onnuri ship was used to obtain acoustic and environmental data. The ship was 68.8 m long and 12.0 m wide, with an international gross tonnage of 1,422 tons. In addition, the ship was equipped with a motion sensor (*i.e.*, Gyro sensor, IXSEA Hydrins) to measure the ship motions, such as pitch (°), roll (°), and heave (m), at every second.

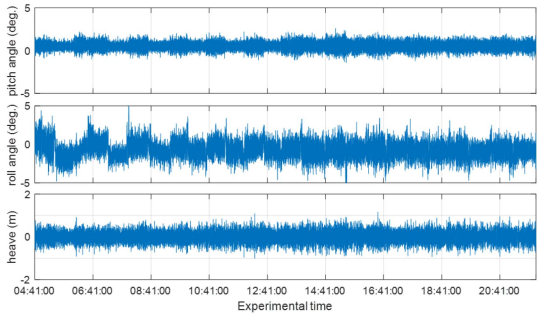

(a) Ship motion measurements (pitch, roll, and heave)

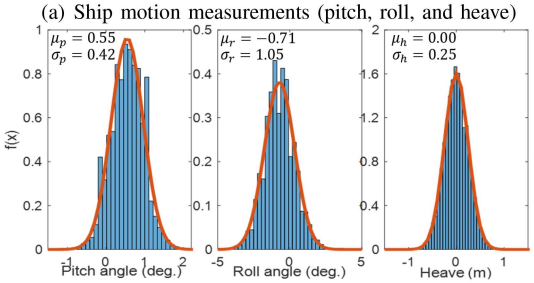

(b) Probability density function (pitch, roll, and heave)

Fig. 4. Ship motion measurements over time in SAVEX15 and its probability density function with Gaussian fitting.

We used subset of the data from SAVEX15, namely MBES2, where the ship moved along the SCAN trajectory (as in Fig. 3). The motion data of MBES2 (as in Fig. 4(a)) was measured from 04:41:00 to 21:55:30 (62,071 samples) on May 18, 2015. In addition, Fig. 4(b) depicts the probability density function of the motion measurement, which exhibits a Gaussian distribution. After we have confirmed that the histogram of the function fitted well to a Gaussian distribution, we represented the pitch and roll angles and heave as Gaussian distributions $N(\mu_p, \sigma_p^2)$, $N(\mu_r, \sigma_r^2)$, and $N(\mu_h, \sigma_h^2)$, respectively. We further extended the measurement model to an oceanic state (OS)-dependent error model based on the Douglas sea scale to augment our simulations for a realistic motion model.

In oceanography, the Douglas sea scale is used to quantitatively describe the OS according to a significant wave height (H_s) level [8], where H_s can be represented as a function of standard deviation of the sea surface elevation (σ_s), *i.e.*, $H_s = 4\sigma_s$ [9]. Because it is difficult to directly obtain the surface elevation measurements on the ship, we used the standard deviation of the measured heave σ_h to approximate σ_s for estimating the wave height (*i.e.*, $H_s \approx 4 \times \sigma_h$).

According to Table I and the measurement of σ_h during MBES2, we confirmed that the MBES2 data were measured in *slight sea* with OS 3. Moreover, it was difficult to obtain the ship motion measurements in extreme weather conditions (*e.g.*, hurricane or typhoon); therefore, we defined a weighted factor

TABLE I
DOUGLAS SEA SCALE [8] AND WEIGHTED FACTORS FOR SIMULATION

Douglas sea scale (OS)	height H_s (m)	probability (%)	w_{os}
1: Calm	0−0.1	5.6243	0
2: Smooth	0.1−0.5	5.6243	0.5
3: Slight	0.5−1.25	31.6851	1.0
4: Moderate	1.25−2.5	40.1944	2.0
5: Rough	2.5−4.0	12.8005	4.0
6: Very Rough	4.0−6.0	3.0253	6.0
7: High	6.0−9.0	0.9263	8.0
8: Very High	9.0−14.0	0.1190	12.0
9: Extreme	+14.0	0.0009	16.0

($w_{os} = \frac{H_s}{4\times\sigma_h}$) to model the pitch and roll angles and to evaluate the performance according to the Douglas sea scale. Based on the calculated w_{os} and wave height with the sea scale, as described in Table I, we modeled the pitch and roll angles and heave with Gaussian distributions $N(\mu_r, (w_{os} \cdot \sigma_r)^2)$, $N(\mu_p, (w_{os} \cdot \sigma_p)^2)$, and $N(\mu_h, (w_{os} \cdot \sigma_h)^2)$, respectively. We assumed that the random values of the motion in time were independent and identical. Even though it was difficult to model the pitch and roll angles owing to the specifications of the ship (*i.e.*, size and weight) and oceanic conditions, such as weather and current [6], [10], the simplified OS-dependent motions can be widely acceptable, according to oceanographic studies [8], [11].

IV. PERFORMANCE EVALUATION

In this section, we evaluate the performance of LMB-MC in comparison with that of LDB [4] and LoMoB [5], in terms of the localization accuracy. We first describe our simulation scenario and the configured parameters. For the simulation, we first considered an environment similar to that of SAVEX15 in a 1 km × 1 km × 100 m three-dimensional (3D) underwater space, where 1000 sensor nodes were randomly deployed. A mobile beacon was used, which was equipped with a directional transceiver and 60° BA and followed a predefined trajectory with a constant beacon distance at a fixed depth. For fair evaluations with the schemes in similar environments, we considered the trajectory as a type of SCAN with a 15 m path interval (PI), and set the mobile beacon (*i.e.*, a ship) movement on the sea surface with a 5 m beacon distance and four reference points ($N = 4$).

To evaluate the accuracy of the schemes, we first define the average location error as $MAE = \frac{1}{n}\sum_{k=1}^{n} \|\hat{\boldsymbol{x}}_{\boldsymbol{k}} - \boldsymbol{x}_{\boldsymbol{k}}\|$, where $\boldsymbol{x}_{\boldsymbol{k}}$ and $\hat{\boldsymbol{x}}_{\boldsymbol{k}}$ are the actual and estimated locations of a sensor node, respectively, and n is the number of deployed sensor nodes. To consider the effect of refraction, we used a Bellhop model with the sound speed profile measured during SAVEX15 [12] and incorporated its irregularities in the radius of the formed beam shape with zero-mean Gaussian distribution $N(0,(\sigma_{rad} = 1 \text{ m})^2)$ as in [5]. To further consider the effect of motion of a mobile beacon, we used the modeled motions from the measurement described in Section III. We performed the simulations in MATLAB.

Figure 5 shows the average location error of the schemes by averaging over 50 simulations according to the Douglas sea scale. As shown in the figure, LMB-MC significantly outperformed LoMoB (*i.e.*, 4.1%−77.6% improvement) and LDB (*i.e.*, 24.1%−89.5%), and the performance gap increased

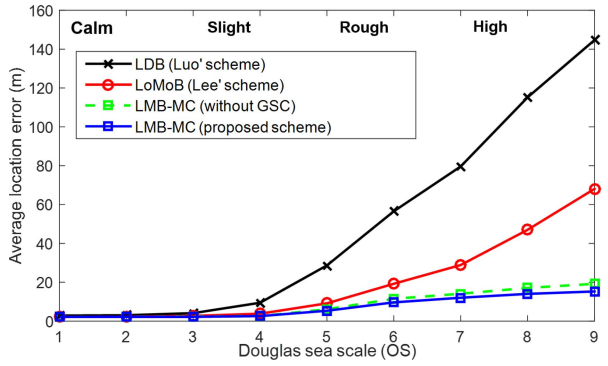

Fig. 5. Location error according to the Douglas scale (d=5 m, $\theta = 60°$).

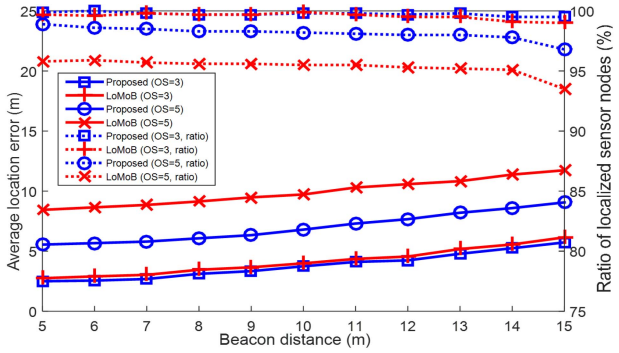

(a) as a function of beacon distance (θ=60°)

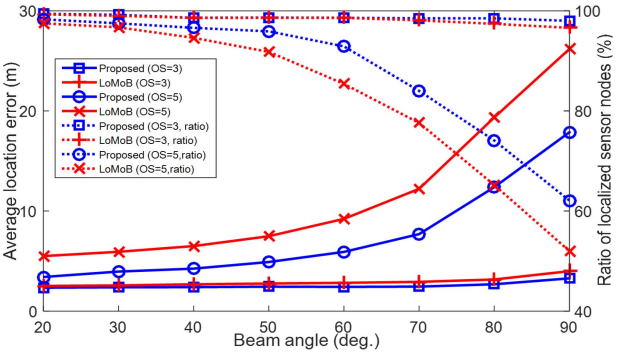

(b) as a function of beam angles (d=5 m)

Fig. 6. Location error and the ratio of localized sensor nodes according to beacon distances and beam angles with oceanic state 3 and 5.

rapidly as the oceanic environment became rough. Moreover, the figure shows that the effect of BPC was more significant than the effect of GSC in the process of LMB-MC. Nonetheless, as the environment gets rough, the performance gap between LMB-MC and LMB-MC without GSC tends to widen (*i.e.*, 1.5%−9.4%). Furthermore, we also evaluated the performance gap with respect to a depth of a deployed sensor node (omitted in the plot due to limitations of space) to clearly confirm the effect of GSC in deep ocean environments (within 1000 m depth). The performance gap increases as the sensor nodes are deployed at a deeper depth (*i.e.*, OS=5, 5.5%−16.3%); therefore, the GSC method should be considered for accurate localization.

As shown in Fig. 6(a), we evaluated the average location error and the ratio of localized sensor nodes with the location

error below 20 m of the schemes with respect to the BDs to confirm that LMB-MC obtained much higher accuracy than LoMoB. LMB-MC attained a higher accuracy compared to LoMoB at a *slight* level (*i.e.*, OS $= 3$, $5.7\%-11.9\%$) and at a *rough* level, (*i.e.*, OS $= 5$, $22.8\%-34.5\%$). The ratio of localized nodes shows a maximum difference of 4.4%. Moreover, as shown in Fig. 6(b), as the BA increases, the performance gap between LMB-MC and LoMoB tends to widen with highly improved accuracy of the former at a *rough* level, (*i.e.*, OS $= 5$, $33.3\%-40.1\%$). Here, the ratio of maximum difference is 10.1%. Throughout the simulations, LMB-MC demonstrated higher reliability in diverse oceanic environments compared with existing range-free schemes.

V. Conclusion

In range-free localization with a mobile beacon, identification of the exact location of sensor nodes is crucial, particularly in harsh oceanic environments. To compensate for the localization errors caused by two uncertainties, i.e., beacon point and geometry uncertainties, we proposed the LMB-MC scheme based on geometric constraints. LMB-MC employs an elliptical model instead of the conventional circle model for geometric constraints, and yields precise localization by significantly improving the accuracy compared to that of the existing solutions. Furthermore, to use realistic motion data, we modeled the pitch, roll, and heave of a mobile beacon based on measurements under oceanic conditions. Simulation results demonstrated that LMB-MC reliably achieved better accuracy compared with existing solutions.

References

[1] Y. Lin, H. Tao, Y. Tu, and T. Liu, "A node self-localization algorithm with a mobile anchor node in underwater acoustic sensor networks," *IEEE Access*, vol. 7, pp. 43773–43780, 2019.

[2] M. Singh, S. Bhoi, and P. Khilar, "Geometric constraint-based range-free localization scheme for wireless sensor networks," *IEEE Sensors J.*, vol. 17, no. 16, pp. 5350–5366, Aug. 2017.

[3] L. Paull, S. Saeedi, M. Seto, and H. Li, "AUV navigation and localization: A review," *IEEE J. Ocean. Eng.*, vol. 39, no. 1, pp. 131–149, Jan. 2014.

[4] H. Luo, Z. Guo, and W. Dong, "LDB: Localization with directional beacons for sparse 3D underwater acoustic sensor networks," *J. Netw.*, vol. 5, no. 1, pp. 28–38, 2010.

[5] S. Lee and K. Kim, "Localization with a mobile beacon in underwater acoustic sensor networks," *Sensors*, vol. 12, no. 5, pp. 5486–5501, 2012.

[6] C. Chen, S. Shiotani, and K. Sasa, "Effect of ocean currents on ship navigation in the east China sea," *Ocean Eng.*, vol. 104, pp. 283–293, Aug. 2015.

[7] H. Song *et al.*, "Shallow-water acoustic variability experiment 2015 (SAVEX15)," Dept. Marine Phys. Lab. Scripps Inst. Oceanography, La Jolla, CA, USA, Rep., Aug. 2015.

[8] F. Tu, S. Ge, Y. Choo, and C. Hang, "Sea state identification based on vessel motion response learning via multi-layer classifiers," *Ocean Eng.*, vol. 147, pp. 318–332, Jan. 2018.

[9] L. Holthuijsen, *Waves in Oceanic and Coastal Waters*. Cambridge, U.K.: Cambridge Univ. Press, 2007.

[10] R. A. Ibrahim and I. M. Grace, "Modeling of ship roll dynamics and its coupling with heave and pitch," *Math. Problems Eng.*, vol. 2010, pp. 1–32, Dec. 2010.

[11] S. Küchler, C. Pregizer, J. K. Eberharter, K. Schneider, and O. Sawodny, "Real-time estimation of a ship's attitude," in *Proc. Amer. Control Conf.*, San Francisco, CA, USA, Jun. 2011, pp. 2411–2416.

[12] Y. Kim, Y. Noh, and K. Kim, "RAR: Real-time acoustic ranging in underwater sensor networks," *IEEE Commun. Lett.*, vol. 21, no. 11, pp. 2328–2331, Nov. 2017.